sciendo

Bio-Algorithms and Med-Systems 2022; 18(1): 158-162

Research article

Dominik Panek*, Monika Szczepanek, Bartosz Leszczyński, Paweł Moskal and Ewa Ł. Stępień

Comparison of Lugol's solution and Fe_3O_4 nanoparticles as contrast agents for tumor spheroid imaging using microcomputed tomography

https://doi.org/10.2478/bioal-2022-0084
Received November 11, 2022; accepted December 11, 2022; published online December 19, 2022.

Keywords: melanoma spheroids, microCT, staining methods, 3D imaging.

Abstract: Background Lugol's solution is well known for its unique contrasting properties to biological samples in in microcomputed tomography imaging. On the other hand, iron oxide nanoparticles (IONPs), which have much lower attenuation capabilities to X-ray radiation show decent cell penetration and accumulation properties, are increasingly being used as quantitative contrast agents in biology and medicine. In our research, they were used to stain 3D cell structures called spheroids. Aim In this study, the micro computed tomography (μCT) technique was used to visualize and compare the uptake and accumulation of two contrast agents, Lugol's solution and iron (II, III) oxide nanoparticles (IONPs) in the in vitro human spheroid tumour model. Methods The metastatic human melanoma cell line WM266-4 was cultured, first under standard 2D conditions, and after reaching 90% confluence cells was seeded in a low adhesive plate, which allows spheroid formation. On the 7th day of growth, the spheroids were transferred to the tubes and stained with IONPs or Lugol's solution and subjected to μCT imaging. Results Our research allows visualization of the regions of absorption at the level of single cells, with relatively short incubation times - 24h - for Lugol's solution. IONPs proved to be useful only in high concentrations (1 mg/ml) and long incubation times (96h). Conclusions When comparing the reconstructed visualizations of the distribution of these stating agents, it is worth noting that Lugol's solution spreads evenly throughout the spheroids, whereas IONPs (regardless of their size 5 and 30 nm) accumulate only in the outer layer of the spheroid structure.

***Corresponding author: D. Panek**, Department of Medical Physics, M. Smoluchowski Institute of Physics, Faculty of Physics, Astronomy and Applied Computer Science, Jagiellonian University ul. Łojasiewicza 11, 30-348 Kraków, Poland; Center for Theranostics, Jagiellonian University ul. Kopernika 40, 31-034 Kraków, Poland; Total-Body Jagiellonian-PET Laboratory, Jagiellonian University, Kraków, Poland, Email: dominik.panek@doctoral.uj.edu.pl
M. Szczepanek, Department of Medical Physics, M. Smoluchowski Institute of Physics, Faculty of Physics, Astronomy and Applied Computer Science, Jagiellonian University ul. Łojasiewicza 11, 30-348 Kraków, Poland; Center for Theranostics, Jagiellonian University ul. Kopernika 40, 31-034 Kraków, Poland; Total-Body Jagiellonian-PET Laboratory, Jagiellonian University, Kraków, Poland
B. Leszczyński, Department of Medical Physics, M. Smoluchowski Institute of Physics, Faculty of Physics, Astronomy and Applied Computer Science, Jagiellonian University ul. Łojasiewicza 11, 30-348 Kraków, Poland; Center for Theranostics, Jagiellonian University ul. Kopernika 40, 31-034 Kraków, Poland
P. Moskal, Department of Medical Physics, M. Smoluchowski Institute of Physics, Faculty of Physics, Astronomy and Applied Computer Science, Jagiellonian University ul. Łojasiewicza 11, 30-348 Kraków, Poland; Center for Theranostics, Jagiellonian University ul. Kopernika 40, 31-034 Kraków, Poland; Total-Body Jagiellonian-PET Laboratory, Jagiellonian University, Kraków, Poland; Department of Experimental Particle Physics and Applications, M. Smoluchowski Institute of Physics, Faculty of Physics, Astronomy and Applied Computer Science, Jagiellonian University, Łojasiewicza 11 St, 30-348 Krakow, Poland
Ewa Ł. Stępień, Department of Medical Physics, M. Smoluchowski Institute of Physics, Faculty of Physics, Astronomy and Applied Computer Science, Jagiellonian University ul. Łojasiewicza 11, 30-348 Kraków, Poland; Center for Theranostics, Jagiellonian University ul. Kopernika 40, 31-034 Kraków, Poland; Total-Body Jagiellonian-PET Laboratory, Jagiellonian University, Kraków, Poland

Introduction

Microcomputed tomography (μCT) is a preclinical imaging method, which allows non-invasive internal

structure visualization with micrometric resolution, exceeding clinical CT by many orders of magnitude [1–4]. Being able to image structures with such resolution gives an opportunity to see in detail different biological structures, even single cells, or cell aggregates [5]. The high contrast in the reconstructed images comes from the differences in densities and atomic (Z) number within the sample. Biological samples are very uniform in terms of density, especially soft tissues. Thus, staining procedures are often used. Staining may be a by-product of a sample preparation, i.e., contamination with heavy metals [6] or could be deliberately done to enhance differences within the sample structure [5,7]. Often such staining agents include Lugol's solution [solution of potassium iodine with iodine in water), which is a common staining agent [8,9]. Lugol's solution is widely used in biological research as a compound that binds carbohydrates, including proteoglycans, and in medical practice as an antibacterial and disinfectant agent [10–13]. Another type of contrasting agents are nanoparticles (NPs), especially AuNPs (gold NPs) or other NPs composed of elements with the high atomic number [14]. The use of iron (II, III) oxide nanoparticles for µCT imaging gains popularity, but it has never been used on a wide scale. Their advantage is high availability and low toxicity [15–17]. Furthermore, IONPs have specific magnetic properties that allow dual imaging, also with nuclear magnetic resonance imaging (MRI) [18,19]. Biological samples, especially on the cellular level, are hard to image due to the similarities in densities. Very accurate models for tumor imaging are spheroids (organoids). They are three-dimensional (3D) cell structures obtained from primary cell cultures and developed to mimic the tissue environment and metabolic activity within *in vitro* conditions [7,20]. Spheroids are a 3D cell culture model, in which the number of cells, nutrients or respiratory conditions [including hypoxia) are better controlled and are the subject of many investigations [5].

In our study, we compared the contrast properties of Lugol's solution and IONPs for use in imaging the structure of human melanoma spheroids in µCT. This approach to tumor imaging is crucial for future research in clinical imaging techniques, where new contrast agents can be conjugated with very specific molecules, i.e. antibodies, and enable the imaging of very specific tumors at a very early stage of development.

Methods

Spheroid culture

The metastatic human melanoma cell line WM266-4 obtained from the ESTDAB Melanoma Cell Bank (Tübingen, Germany) was used. Cells were cultured in RPMI 1640 medium (Cat. No. 21875091 Gibco™ Paisley, UK) supplemented with 10% fetal bovine serum (Cat. No. 10500064 Gibco™ Paisley, UK), 100 U/mL penicillin and 100 µg/mL streptomycin (at. No. 15140122 Gibco™), 2mM L-glutamine (Cat. No. 25030081 Gibco™ Paisley, UK), seeded into a T75cm2 flask and incubated at 37°C in a humidified atmosphere of 5% CO2. After reaching the confluence of 90%, cell cultures were washed with PBS w/o Ca^{2+}, Mg^{2+} (Cat. No. 10010056 Gibco™ Paisley, UK), trypsinized (Trypsin – EDTA, Cat. No. 25200072 Gibco™ Paisley, UK) to obtain single cell suspension. Then cells were then stained with trypan blue dye and counted using an automatic cell counter (Luna II). The given number of cells was seeded on a 96-well low adhesive plate (SPL 3DTM Cell Floater Plate), 2,000 cells were placed in each well to form a spheroid. Culture medium was replaced every second day.

Staining

The culture of spheroids, staining procedure, and imaging workflow is presented in Fig. 1. On day 6 of spheroid growth, two types of functionalized by polyethene glycol (PEG) IONPs: 5 nm (Cat. No., 790508-10ML, Sigma Aldrich) and 30 nm (Cat. No. 747408-10ML, Sigma Aldrich) were added in concentrations of 1 mg/ml. Other spheroids were stained with Lugol's solution (Cat. No. L6146, Sigma Aldrich) in concentration of 10% (total concentration of iodine 25.3 mg/100 µl). After 96 h of incubation, all IONP-stained spheroids were transferred into the Eppendorf tubes, washed, and prepared for µCT. Visualization of Lugol-stained spheroids was performed after 24 h of incubation.

Imaging

The Skyscan 1172 microtomograph (Bruker) with 8W X-ray tube was used for µCT imaging (Fig. 1C). The imaging parameters were as follows: voltage at 33 kV, amperage at 100 µA, rotation step 0.15 deg, and the size of the image pixel ranged from 2.9 to 5 µm. The number of resulting

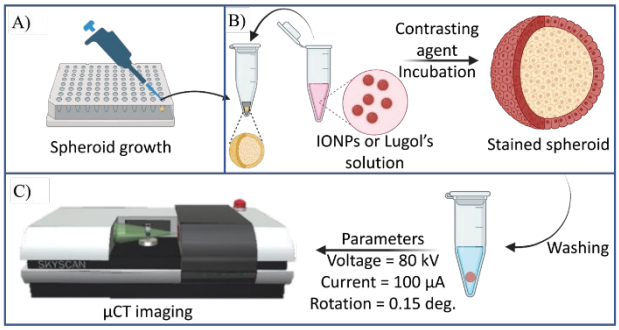

Figure 1: Sample preparation workflow. From the top: A) Spheroid formation, and growth in the low-adhesive 96-well plate, B) Staining procedure with IONPs or Lugol's solution. C) After staining, the spheroid was washed three times. Afterwards, the imaging parameters were set and the imaging began. Figure created with BioRender.com.

pixel ranged from 2.9 to 5 µm. The number of resulting projections ranged from 1,500 to 2,000.

Reconstruction

Image reconstruction was performed with NRecon software (Skyscan, Bruker µCT, version 1.7.3.1). These parameters include misalignment compensation or dynamic range (DR). The first one accounts for the minimalization of the artifacts resulting from the physical characteristics of the measurement (small movements due to the long time of imaging). Another one allowed to map the greyscale values to be identical for all the samples. The lower boundary of the DR was set to exclude air from the images and the upper was set to the maximal value registered during the measurement with Lugol's solution.

Visualization

Visualization was performed with two softwares: CTAnalyzer (Skyscan, Bruker micro-CT, version 1.16.1.0) and CTVox (Skyscan, Bruker micro-CT, version 3.3.0 r1403). CTAnalyzer was used to choose the region of interest (ROI) from all reconstructed images within a given sample. After ROI selection, the volume of interest (VOI) was created as the read-in data saved for every sample and analyzed by CTVox. It enabled to visualize results using the technique called volume rendering. Transfer functions (TFs) were used to map the grayscale values to the RGB (red-green-blue) color scale. Additionally, the TF opacity was used to eliminate the noise produced during data reconstruction.

Results and discussion

Reconstructed and rendered images are presented in the Fig. 2. In the spheroids stained with both types of IONPs the accumulation was observed in the outer layer of the spheroid structure (Fig. 2A, 2B), no penetration to the inner structure is visible. There are also differences in the distributions for the two types of nanoparticles in different size. The bigger the nanoparticle size, the smoother and more uniform its distribution on the reconstructed images is. Smooth distribution can be seen in Fig. 2A, and more ununiform is visible in Fig. 2B. However, a completely different properties of the staining agent can be seen for the spheroid incubated with Lugol's solution. The uptake of this staining agent is uniform throughout the structure (Fig. 2C). These differences can be the result of the fact that iodine in Lugol's solution

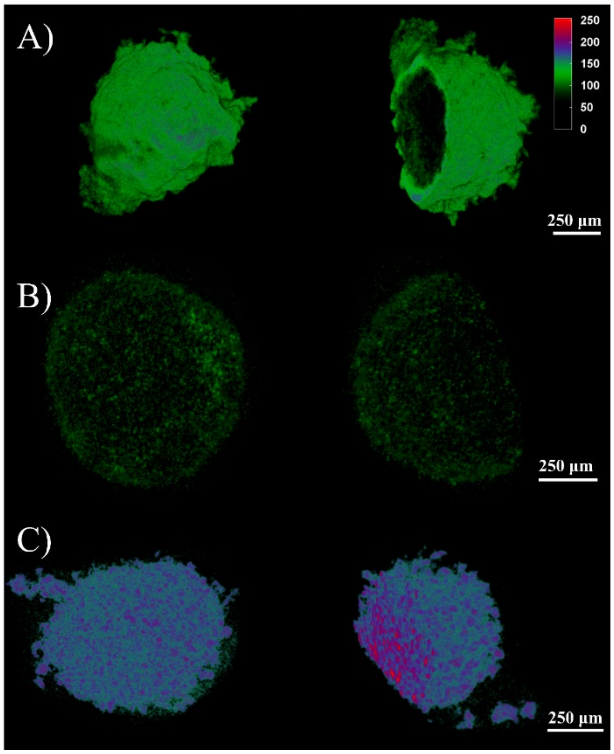

Figure 2: Reconstructed images of spheroids cultured from the WM-266-4 cell line. The left column shows entire spheroids, while the right column represents the cross section through the structures to reveal the inner structure and the uptake of the staining agents. A) Spheroid stained with 1 mg/ml of 30 nm IONPs for 96h. B) Spheroid stained with 1 mg/ml of 5 nm IONPs for 96h. C) Spheroid stained using Lugol's solution for 24 h. The color bar in the corner represents density scale. Green corresponds to the lower density, and red corresponds to the higher density in the spheroids.

occurs in an ionic form, which facilitates the diffusion, whereas IONPs occur in neutral form. However, the uptake of IONPs is probably also facilitated by the PEGylation of their structure. Considering that the incubation time for IONPs requires 96 h and the minimum concentration of 1 mg/ml, it would be problematic for them to compete with the standard, traditionally used iodine, where 24 h incubation is enough to obtain much more distinctive images. Some studies already proved IONPs to be unable to deliver enough contrast, however, lower resolutions and NPs with much larger diameters were used [21]. In order to increase the contrast, some authors suggest that the mixtures of gold NPs and IONPs can be used. Furthermore, it would not only facilitate dual imaging but would also reduce the cost of using only gold NPs [22].

Conclusions

Our studies show the usefulness of the common contrast agent, which is Lugol's solution. The high atomic number of iodine present in this staining reagent to see clear and very well-defined structures in the reconstructed images (Fig. 2C). Furthermore, the short incubation time favors the overall application of this staining agent. IONPs deliver the required contrast after long incubation times and a high concentration applied (96h, and 1 mg/ml in both NPs, respectively), which limits their utility in the case of micro-CT imaging. Reportedly, nanoparticles with higher atomic number (i.e., gold NPs) would perform even better in much lower concentrations and times of incubation.

Nevertheless, obtaining such a crisp and clear image of spheroids proves that micro-CT can be a very powerful tool for spheroid imaging. Not only nanoparticle localization but also the intensity of the accumulation process can be visualized. In the future, staining agents conjugated to tumor-specific antibodies would even allow for visualization of sites of increased receptor expression.

Acknowledgements

The authors are grateful to Prof. J. Chwiej for kind sharing of IOPNs. The authors acknowledge the support by the TEAM POIR.04.04.00-00-4204/17 program, the SciMat and qLife Priority Research Areas budget under the program Excellence Initiative - Research University at the Jagiellonian University and by DSC grant, no. N17/MNS/000058/2021 awarded to D. Panek and funded by Jagiellonian University.

References

[1] Leszczyński B, Skrzat J, Kozerska M, Wróbel A, Walocha J. Three dimensional visualisation and morphometry of bone samples studied in microcomputed tomography (micro-CT). Folia Morphol. 2014;73(4):422-428.

[2] Leszczyński B, Sojka-Leszczyńska P, Wojtysiak D, Wróbel A, Pędrys R. Visualization of porcine eye anatomy by X-ray microtomography. Exp Eye Res. 2018;167:51-55.

[3] Stauber M, Müller R. Micro-computed tomography: a method for the non-destructive evaluation of the three-dimensional structure of biological specimens. Methods Mol Biol. 2008;455:273-292.

[4] Forrest LJ. Computed Tomography Imaging in Oncology. Vet Clin North Am Small Anim Pract. 2016;46(3):499.

[5] Karimi H, Leszczyński B, Kołodziej T, Kubicz E, Przybyło M, Stępień E. X-ray microtomography as a new approach for imaging and analysis of tumor spheroids. Micron [Internet] 2020;137:102917.

[6] Panek D, Leszczyński B, Wojtysiak D, Drąg-Kozak E, Stępień E. Micro-computed tomography for analysis of heavy metal accumulation in the opercula. Micron [Internet]. 2022;160:103327. Available from: https://www.sciencedirect.com/science/article/pii/S0968432822001238

[7] Stępień E, Karimi H, Leszczyński B, Szczepanek M. Melanoma Spheroids as a Model for Cancer Imaging Study. Acta Physica Polonica. B 51, 2020:159–63.

[8] Xia CW, Gan RL, Pan JR, et al. Lugol's Iodine-Enhanced Micro-CT: A Potential 3-D Imaging Method for Detecting Tongue Squamous Cell Carcinoma Specimens in Surgery. Front Oncol. 2020;10:550171.

[9] Dawood Y, Hagoort J, Siadari BA, Ruijter JM, Gunst QD, Lobe NHJ, et al. Reducing soft-tissue shrinkage

artefacts caused by staining with Lugol's solution. Sci Rep. 2022;12(1):2366

[10] Gottardi W. Iodine and disinfection: theoretical study on mode of action, efficiency, stability, and analytical aspects in the aqueous system. Arch Pharm (Weinheim). 1999;332(5):151-157.

[11] Mantlo E, Evans A, Patterson-Fortin L, Boutros J, Smith R, Paessler S. Efficacy of a novel iodine complex solution, CupriDyne, in inactivating SARS-CoV-2. 2020.05.08 [Epub ahead of print].

[12] Leyssens L, Pestiaux C, Kerckhofs G. A Review of Ex Vivo X-ray Microfocus Computed Tomography-Based Characterization of the Cardiovascular System. Int J Mol Sci. 2021;22(6):3263.

[13] De Bournonville S, Vangrunderbeeck S, Kerckhofs G. Contrast-Enhanced MicroCT for Virtual 3D Anatomical Pathology of Biological Tissues: A Literature Review. Contrast Media Mol Imaging. 2019;2019:8617406.

[14] Ashton JR, West JL, Badea CT. In vivo small animal micro-CT using nanoparticle contrast agents. Frontiers in Pharmacology. 2015;6:1663-9812.

[15] Alphandéry E., Iron oxide nanoparticles as multimodal imaging tools, RSC Adv., 2019;9:40577-40587.

[16] Janik-Olchawa N, Drozdz A, Ryszawy D, Pudełek M, Planeta K, Setkowicz Z, et al. Comparison of ultrasmall IONPs and Fe salts biocompatibility and activity in multi-cellular in vitro models. Sci Rep. 2020;10(1).

[17] Drozdz A, Matusiak K, Setkowicz Z, et al. FTIR microspectroscopy revealed biochemical changes in liver and kidneys as a result of exposure to low dose of iron oxide nanoparticles. Spectrochim Acta A Mol Biomol Spectrosc. 2020;236:118355.

[18] Crețu BE, Dodi G, Shavandi A, Gardikiotis I, Șerban IL, Balan V. Imaging Constructs: The Rise of Iron Oxide Nanoparticles. Molecules. 2021;26(11):3437.

[19] Wabler M, Zhu W, Hedayati M, et al. Magnetic resonance imaging contrast of iron oxide nanoparticles developed for hyperthermia is dominated by iron content. Int J Hyperthermia. 2014;30(3):192-200.

[20] Stępień E. Factors influencing neurite outgrowth in vitro [Ph. D. thesis]. Kraków Jagiellonian University; 1999.

[21] Hoopes PJ, Petryk AA, Gimi B, et al. In Vivo Imaging and Quantification of Iron Oxide Nanoparticle Uptake and Biodistribution. Proc SPIE Int Soc Opt Eng. 2012;8317:83170.

[22] Lamichhane N, Sharma S, Parul, Verma AK, Roy I, Sen T. Iron Oxide-Based Magneto-Optical Nanocomposites for In Vivo Biomedical Applications. Biomedicines. 2021;9(3):288.